Advanced Review

Umbrella sampling

Johannes Kästner*

The calculation of free-energy differences is one of the main challenges in computational biology and biochemistry. Umbrella sampling, biased molecular dynamics (MD), is one of the methods that provide free energy along a reaction coordinate. Here, the method is derived in a historic overview and is compared with related methods like thermodynamic integration, slow growth, steered MD, or the Jarzynski-based fast-growth technique. In umbrella sampling, bias potentials along a (one- or more-dimensional) reaction coordinate drive a system from one thermodynamic state to another (e.g., reactant and product). The intermediate steps are covered by a series of windows, at each of which an MD simulation is performed. The bias potentials can have any functional form. Often, harmonic potentials are used for their simplicity. From the sampled distribution of the system along the reaction coordinate, the change in free energy in each window can be calculated. The windows are then combined by methods like the weighted histogram analysis method or umbrella integration. If the bias potential is adapted to result in an even distribution between the end states, then this whole range can be spanned by one window (adaptive-bias umbrella sampling). In this case, the free-energy change is directly obtained from the bias. The sampling in each window can be improved by replica exchange methods; either by exchange between successive windows or by running additional simulations at higher temperatures. *WIREs Comput Mol Sci* 2011 1 932–942 DOI: 10.1002/wcms.66

INTRODUCTION

The calculation of free-energy differences is a central task in computational science. The free-energy difference is the driving force of any process, such as a chemical reaction. Transition state theory[1–3] can be used to calculate reaction rates from energy barriers, more exactly free-energy barriers.[4] The free energy contains the entropy, a measure for the available space. To map the available space in a system bigger than a few atoms, extensive sampling is required.[5,6] Techniques are regularly being reviewed in the literature, with a few recent ones given in *J Comput Chem*[7] and in a themed issue of *J Comput Chem* in 2009.[8,9] Applications range from the solid state, catalytic reactions, biochemical processes to rational drug design.

The canonical partition function Q of a system can be calculated via an integral over the whole phase space, i.e., configuration space and momentum space. If the potential energy E is independent of the momentum, the integral over the latter is a multiplicative constant to Q, which can be ignored. Then, Q is obtained as

$$Q = \int \exp[-\beta\, E(r)] d^N r \qquad (1)$$

with $\beta = 1/(k_B T)$, k_B being the Boltzmann's constant, T being the absolute temperature, and N being the number of degrees of freedom of the system.

The free (Helmholtz) energy A is related to Q via $A = -1/\beta \ln Q$. The canonical partition function involves a constant number of particles, constant volume, and a constant temperature. If the pressure, rather than the volume, is kept constant, the Gibbs free energy (usually denoted as G) is obtained. Apart from the change in the ensemble, the following formalisms and derivations are equivalent for A and G. In the condensed phase, which is relevant for most applications, the systems are hardly compressible; so ΔA and ΔG are numerically very similar.

In chemical reactions, one is generally interested in free-energy differences between two states. If the two states differ by geometry (like a reactant and product of a reaction) then the integration in Eq. (1) is done over a part of the coordinate space for each state.

In many cases, a reaction coordinate (ξ), a continuous parameter which provides a distinction

*Correspondence to: kaestner@theochem.uni-stuttgart.de

Computational Biochemistry Group, Institute of Theoretical Chemistry, University of Stuttgart, Stuttgart, Germany

DOI: 10.1002/wcms.66

between two thermodynamic states, can be defined. Any order-parameter is possible, even a change in the energy expression (the Hamiltonian). The reaction coordinate can be one or more dimensional. Often, ξ is defined on geometric grounds, such as distance, torsion, or the difference between root mean square deviations from two reference states.

With ξ defined, the probability distribution of the system along ξ can be calculated by integrating out all degrees of freedom but ξ:

$$Q(\xi) = \frac{\int \delta[\xi(r) - \xi] \ \exp[(-\beta E) d^N r]}{\int \exp[(-\beta E) d^N r]}. \qquad (2)$$

$Q(\xi)\,\mathrm{d}\xi$ can be interpreted as the probability of finding the system in a small interval $\mathrm{d}\xi$ around ξ. Consequently, this allows the calculation of the free energy along the reaction coordinate; $A(\xi) = -1/\beta \ln Q(\xi)$. $A(\xi)$ is also called potential of mean force (PMF). If ξ is a general, i.e., non-Cartesian, coordinate, or a set of those, a Jacobian term enters Eq. (2). As long as the integration is performed in Cartesian coordinates, $Q(\xi) = \int \delta[\xi(r) - \xi] \exp(-\beta E)\ d^N r/Q$. If the integration is done in a different set of coordinates, q, ξ being one of those, an explicit Jacobian determinant $|J(q)|$, with $J_{ij} = \mathrm{d}q_i/\mathrm{d}r_j$, has to be taken into account: $Q(\xi) = \int \exp(-\beta E)|J(q)|d^{N-1}q/Q$, where the integration is performed over all coordinates except ξ.

In computer simulations, the direct phase-space integrals used in Eqs. (1) and (2) are impossible to calculate. However, if the system is ergodic, i.e., if every point in phase space is visited during the simulation, $Q(\xi)$ is equal to

$$P(\xi) = \lim_{t\to\infty} \frac{1}{t} \int_0^t \rho[\xi(t')]\mathrm{d}t' \qquad (3)$$

that is, the ensemble average $Q(\xi)$ becomes equal to the time average $P(\xi)$ for infinite sampling in an ergodic system. In Eq. (3), t denotes the time and ρ simply counts the occurrence of ξ in a given interval (of infinitesimal width in the exact equation and of finite width when calculating a histogram). So, in principle, $A(\xi)$ can be directly obtained from molecular dynamics (MD) simulations by monitoring $P(\xi)$, the distribution of the system along the reaction coordinate.

Note that the terms distribution, distribution function, frequency, probability density, and possibly a few more are sometimes used in the literature of chemistry and physics in different contexts. Throughout this article, the term distribution $P(\xi)$ refers to the normalized frequency of finding the system in the vicinity of a given value of ξ. If $P(\xi)$ was obtained from an exact ensemble average rather than a sampled quantity, $P(\xi)$ would refer to a probability density.

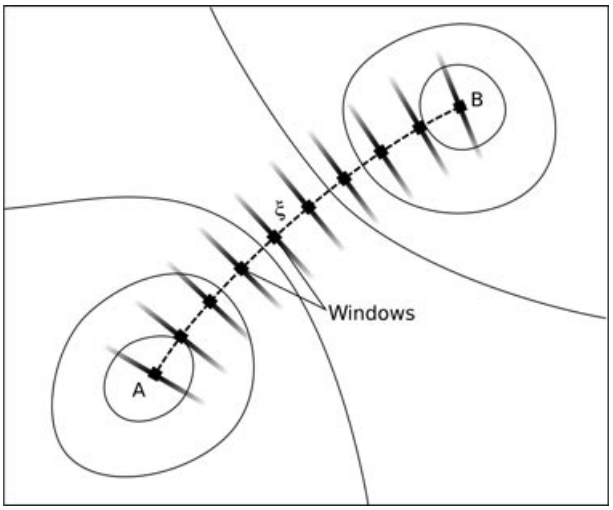

FIGURE 1 | Separation of the reaction coordinate (dashed line) between two states (here represented by two minima on the potential energy surface) into distinct windows. The system is mainly sampled perpendicular to the reaction coordinate in each window.

However, simulations are only run for finite time. Regions in configuration space around a minimum in $E(r)$ are typically sampled well, whereas regions of higher energy are sampled rarely. For rare events, those with an energy barrier significantly larger than $k_B T$, direct sampling is infeasible. To obtain a profile $A(\xi)$, however, also those high-energy regions, those rare events, are required.

Different techniques have been developed to sample such rare events. One can broadly distinguish three different families of methods: (1) methods that sample the system in equilibrium, (2) nonequilibrium sampling techniques, and (3) methods that introduce additional degrees of freedom, along which the free energy is calculated. The third family includes λ-dynamics[9–12] and metadynamics.[13] The latter is covered in a different contribution in this series and will not be discussed here.

In the remaining two families of methods, global sampling can be approximated by two techniques, schematically illustrated in Figure 1. On the one hand, the path is split into windows. Each window covers only a small part of the range of ξ. The windows are sampled individually. In postprocessing, the results of the different windows are combined to result in a global free-energy profile $A(\xi)$. On the other hand,

one can run multiple simulations. In each of those, the system is driven from one state of interest (A) to the other state (B), taking a different path each time. The postprocessing in this case includes averaging over the different simulations.

This review is organized as follows. In *Accelerated Sampling Techniques*, the context of umbrella sampling is described by briefly introducing different techniques to sample free-energy profiles in MD simulations. In *Umbrella Sampling: Method*, the methodical details of umbrella sampling are derived and described. *Bias Potentials* deals with different bias potentials, whereas *Sampling Techniques* mentions techniques to accelerate the MD sampling itself. *Methods to Analyze Umbrella Sampling Simulations* discusses the most common methods to analyze umbrella sampling simulations, i.e., to extract a free-energy profile from the sampled data. *Conclusion* finally summarizes the topic.

ACCELERATED SAMPLING TECHNIQUES

Accelerated Sampling Techniques Based on Equilibrium Properties

All of the acceleration techniques discussed in this review have the goal of calculating the free-energy difference, an equilibrium property. However, in each simulation, the system can either be in equilibrium, or one can measure the response to some perturbation and derive the free-energy change from that. The former case will be discussed here, the latter in *Free-Energy Differences from Nonequilibrium Simulations*.

To drive a system over an energy barrier, one can either (1) modify the energy expression in order to reduce the barrier, or (2) restrict the sampling space to all degrees of freedom, but the reaction coordinate describing the transition over the barrier. The former is known as biased MD or umbrella sampling.[14,15] Because this is the main focus of the present review, it will be discussed in detail in *Umbrella Sampling: Method*.

In *thermodynamic integration*,[16–21] a technique sometimes also referred to as blue moon sampling,[18,22] the transition over a barrier is simulated by freezing the reaction coordinate at different values in a number of windows and sampling the system perpendicular to ξ. The constraint freezing the reaction coordinate has to be implemented in an energy-conserving manner. Generally, the method of Lagrange multipliers (Shake algorithm[23]) is used. The force on the frozen reaction coordinates is sampled. The resulting *mean force* is the derivative of the free energy with respect to the reaction coordinate. Integration of the mean force results in the PMF.

It should be noted that there is some confusion in the older literature over the term PMF.[24] Especially in the field of thermodynamic integration, one often referred to PMF as a quantity directly obtained by integrating the mean force, which differs from the free energy by neglect of a correction of the metric tensor. If the reaction coordinate is a spatial coordinate or a combination of those, constraining it to a fixed value also changes the momentum sampling. There is one component of the momentum canonically conjugated to each component of the spatial coordinates. If ξ is frozen, the associated momentum is frozen (zero) as well. This can lead to a change in the metric tensor of the system. For simple reaction coordinates, metric-tensor corrections have been derived.[21,25–31]

Rather than keeping the reaction coordinate fixed in a number of windows, one can also vary a constraint slowly from one state to another in an approach termed *slow growth*.[32–34] Average and integration of the force on the constraint results in the free energy.

In umbrella sampling,[14,15] the reaction coordinate is not constrained, but only restrained and pulled to a target value by a bias potential. Therefore, the full momentum space is sampled. Usually, umbrella sampling is done in a series of windows, which are finally combined either with the weighted histogram analysis method (WHAM)[35,36] or using umbrella integration.[37]

The bias potential can be varied to pull the system from one state to another rather than keeping it fixed. If that variation is slow as compared with the relaxation time of the system, the analysis can be performed by assuming an equilibrium state of the system, i.e., the mean force on the reaction coordinate can be sampled and integrated. This approach gained popularity under the name of *steered MD* (SMD).[38–41] SMD directly simulates the influence of an atomic-force microscope cantilever acting, e.g., on a protein.

Free-Energy Differences from Nonequilibrium Simulations

Jarzynski[42] demonstrated the equivalence of the free-energy change and an exponential average over the work W along nonreversible paths originating from a canonic ensemble:

$$\exp(-\beta \Delta A) = \langle \exp(-\beta W) \rangle. \quad (4)$$

This can be exploited in practical simulations by moving a constraint on the reaction coordinate relatively fast from an equilibrated system to the target system.[43,44] This method became known as *fast growth*. It is related to Bennett's acceptance ratio method.[45] The changes in the energy along these paths are averaged according to Eq. (4). The computational tradeoff is that the faster the constraint is varied, the larger is the statistical spread, and thus, more trajectories have to be calculated.

Free-energy perturbation[46] (FEP) can be regarded as a limiting case of methods based on Jarzynski's equation:

$$\exp(-\beta\Delta A) = \langle \exp(-\beta\Delta E)\rangle_a \tag{5}$$

with ΔE being the difference of the initial state and the final state, and the ensemble averaged over the initial state a. It should be noted, of course, that FEP was proposed and used many decades before the more general Eq. (4). In FEP, the instantaneous change from one state to another is sampled over a canonical ensemble. Thus, it corresponds to fast growth with the constraint immediately moved to the target value. The exponential average of the change results in the free-energy difference. The term 'perturbation' is misleading because the method is exact and does not correspond to a perturbation theory in the usual sense.

A special challenge for free-energy simulations are quantum mechanics/molecular mechanics (QM/MM) setups, in which a small part of the system is described by comparatively expensive QM calculations, whereas most of the system is handled by classical force fields (MM).[47] A variant of FEP[48–50] can be used to restrict the sampling to the computationally cheaper force field part.

UMBRELLA SAMPLING: METHOD

Umbrella sampling was developed by Torrie and Valleau[14,15] based on related previous work.[51,52] A bias, an additional energy term, is applied to the system to ensure efficient sampling along the whole reaction coordinate. This can either be aimed at in one simulation or in different simulations (windows), the distributions of which overlap. The effect of the bias potential to connect energetically separated regions in phase space gave rise to the name umbrella sampling.

In this section, the formalism of recovering unbiased free-energy differences from biased simulations will be discussed. The next section describes different forms of bias potentials used in the literature.

The bias potential w_i of window i is an additional energy term, which depends only on the reaction coordinate:

$$E^{\mathrm{b}}(r) = E^{\mathrm{u}}(r) + w_i(\xi). \tag{6}$$

The superscript 'b' denotes biased quantities, whereas the superscript 'u' denotes unbiased quantities. Quantities without superscripts are always unbiased.

In order to obtain the unbiased free energy $A_i(\xi)$, we need the unbiased distribution, which is, according to Eq. (2):

$$P_i^{\mathrm{u}}(\xi) = \frac{\int \exp[-\beta E(r)]\ \delta[\xi'(r) - \xi]\ d^N r}{\int \exp[-\beta E(r)]\ d^N r}. \tag{7}$$

MD simulation of the biased system provides the biased distribution along the reaction coordinate P_i^{b}. Assuming an ergodic system,

$$P_i^{\mathrm{b}}(\xi) = \frac{\int \exp\{-\beta[E(r) + \omega_i(\xi'(r))]\}\delta[\xi'(r) - \xi]d^N r}{\int \exp\{-\beta[E(r) + \omega_i(\xi'(r))]\}d^N r}. \tag{8}$$

Because the bias depends only on ξ and the integration in the enumerator is performed over all degrees of freedom but ξ,

$$P_i^{\mathrm{b}}(\xi) = \exp[-\beta\omega_i(\xi)] \times \frac{\int \exp[-\beta E(r)]\delta[\xi'(r) - \xi]d^N r}{\int \exp\{-\beta[E(r) + \omega_i(\xi'(r))]\}d^N r}. \tag{9}$$

Using Eq. (7) results in

$$\begin{aligned} P_i^{\mathrm{u}}(\xi) &= P_i^{\mathrm{b}}(\xi)\ \exp[\beta\omega_i(\xi)] \times \frac{\int \exp\{-\beta\,[E(r) + \omega_i\,(\xi(r))]\}\,d^N r}{\int \exp\,[-\beta E(r)]\,d^N r} \\ &= P_i^{\mathrm{b}}(\xi)\ \exp[\beta\omega_i(\xi)] \times \frac{\int \exp[-\beta E(r)]\ \exp\{-\beta\,\omega_i[\xi(\vec{r})]\}d^N r}{\int \exp[-\beta E(r)]d^N r} \\ &= P_i^{\mathrm{b}}(\xi)\ \exp[\beta\omega_i(\xi)]\,\langle \exp[-\beta\omega_i(\xi)]\rangle. \end{aligned} \tag{10}$$

From Eq. (10), $A_i(\xi)$ can be readily evaluated. $P_i^{\mathrm{b}}(\xi)$ is obtained from an MD simulation of the biased system, $w_i(\xi)$ is given analytically, and $F_i = -(1/\beta)\ \ln\langle \exp[-\beta\,\omega_i(\xi)]\rangle$ is independent of ξ:

$$A_i(\xi) = -(1/\beta)\ \ln P_i^{\mathrm{b}}(\xi) - w_i(\xi) + F_i. \tag{11}$$

This derivation is exact. No approximation enters apart from the assumption that the sampling in each window is sufficient. This is facilitated by an appropriate choice of umbrella potentials $w_i(\xi)$.

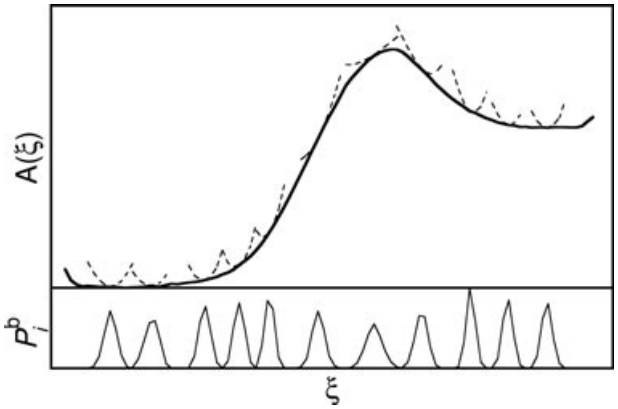

FIGURE 2 | Global free energy (thick solid curve) and the contributions A_i of some of the windows (thin dashed curves). For clarity, only every third window is shown. At the bottom, the biased distributions P_i^b as obtained from the simulation are shown (thin solid curves). Relatively few bins (100) have been used to generate this figure.

As long as one window spans the whole range of ξ to be studied, Eq. (11) is sufficient to unbias the simulation. $A(\xi)$ is in any case only defined up to an additive constant; so in this case, F_i can be chosen arbitrarily.

If the free-energy curves $A_i(\xi)$ of more windows are to be combined to one global $A(\xi)$, see Figure 2, the F_i have to be calculated. They are associated with introducing the bias potential and connect the free-energy curves $A_i(\xi)$ obtained in the different windows:

$$\begin{aligned}\exp(-\beta F_i) &= \langle \exp[-\beta\, \omega_i(\xi)] \rangle \\ &= \int P^u(\xi) \exp[-\beta\, \omega_i(\xi)] d\xi \\ &= \int \exp\{-\beta[A(\xi) + \omega_i(\xi)]\} d\xi \end{aligned} \quad (12)$$

with $P^u(\xi)$ being the global unbiased distribution. The F_i cannot directly be obtained from sampling. *Methods to Analyze Umbrella Sampling Simulations* will deal with methods to calculate them, i.e., to combine the results of different windows in umbrella sampling.

BIAS POTENTIALS

Ideally, the bias potential is chosen such that sampling along the whole range of the reaction coordinate ξ is uniform. Therefore, the optimal bias potential is $w_{opt} = -A(\xi)$. This would lead to a truly uniform distribution $P_i^b(\xi)$. However, $A(\xi)$ is obviously not known; it is what we aim to calculate with umbrella sampling. Therefore, two main families of bias potentials have emerged: harmonic biases in a series of windows along ξ, and an adaptive bias, which is adjusted to match $-A(\xi)$ in only one window spanning the whole range of ξ.

Harmonic Bias Potentials

To ensure sampling in all regions of ξ, the range of interest of ξ is split into a number of windows. In each window, a bias function is applied to keep the system close to the reference point ξ_i^{ref} of the respective window i. Often, a simple harmonic bias of strength K is used:

$$\omega_i(\xi) = K/2\left(\xi - \xi_i^{ref}\right)^2. \quad (13)$$

After the simulations, the free-energy curves are combined with techniques discussed in *Methods to Analyze Umbrella Sampling Simulations* (typically WHAM or umbrella integration). The form of the bias given in Eq. (13) is appealing because it contains only few parameters: K (which in principle can be window dependent), the number of images, and ξ_i^{ref}. The latter are usually chosen uniformly distributed along ξ. The higher the number of images, the smaller is generally the statistical error relative to CPU time.[53] However, the CPU time needed for equilibration, on the contrary, increases with the number of images. The MD simulations of the images are completely independent and thus, can run in parallel.

The choice of K, the strength of the bias, is the only critical decision. It has to be made before simulations are run. By contrast, additional windows could always be inserted if the first series of windows results in too large gaps between the distributions. Overall, K has to be large enough to drive the system over the barrier. Too large K, however, will cause very narrow distributions $P_i^b(\xi)$. Sufficient overlap between the distributions is required for WHAM, whereas it is not required, but still advantageous in umbrella integration.[54] Increasing K at constant time step also leads to increasing errors in the numerical integration of the equations of motions. If the time step is too large (or K is too large), configurations with high energies will be overrepresented.[20]

For umbrella integration analysis, analytic expressions for the statistical error can be derived, which allow an estimate of an ideal K based on quantities, which can often be estimated prior to sampling.[54] It has also been suggested that the location of the next window to be sampled ($\xi_{i+1}{}^{ref}$) can be chosen from the location and the widths of the previous

window to match their estimated half maxima.[55] An alternative is to use data from the experiment to define the most promising bias parameters.[56]

Adaptive Bias Umbrella Sampling

The aim of adaptive bias umbrella sampling[13,57–60] is to cover the whole range of interest of the reaction coordinate ξ in one simulation. In principle, this can be achieved by choosing a bias $w(\xi) = -A(\xi)$. This exactly flattens the energy surface and leads to a uniform sampling along ξ. Because $A(\xi)$ is, of course, not known *a priori*, one typically starts out with an initial guess of $w(\xi)$ and iteratively improves it to achieve a uniform distribution.

Specialized Umbrella Potentials

The local elevation method[61] adds, similar to metadynamics, a history-dependent (and thus, time-dependent) bias to the potential energy. This has recently[62,63] been combined with umbrella sampling by building up a local elevation bias in a comparatively short simulation and then sampling the distribution in that bias to reconstruct the free energy. Other special forms of umbrella potentials were used.[64]

SAMPLING TECHNIQUES

In each window of an umbrella sampling run, the phase space has to be sampled as good as possible. Overlap between windows is required for WHAM analysis (see below) and is desirable for umbrella integration. The quality of the sampling can be enhanced by Hamiltonian replica exchange.[65–67] In specified intervals, the geometry of window i is used to calculate the total biased energy of a neighboring window j (i.e., the bias w_j of window j is used), and additionally, the energy of geometry j with the bias w_i is calculated. If the sum of these energies is smaller than the sum of the original energies, the two sets of coordinates are exchanged. If the sum is larger, exchange is still possible based on the Metropolis criterion. Then the simulations continue. This is done at regular intervals with all pairs of images. Replica exchange between umbrella sampling windows enhances the quality of the sampling without additional computational cost.

The better the sampling, the more important is a proper choice of the reaction coordinate. If the reaction coordinate misses important structural changes, it can lead to artificial lowering or raising of the result obtained by umbrella sampling.[8] A too high barrier may be the result of an unfavorable path being taken. A too low barrier may be the result of discontinuities in the path: the change from one window i to the next window $i+1$ may be reflected by only a small change in ξ, but a larger change in other degrees of freedom which are not included in ξ. Such artificial behavior results in jumps in the root mean square difference between the average structures of subsequent umbrella sampling windows.[8]

METHODS TO ANALYZE UMBRELLA SAMPLING SIMULATIONS

Weighted Histogram Analysis Method (WHAM)

Numerous methods have been proposed for an estimation of F_i,[68,69] a promising one being[70] the WHAM.[35,36] It aims to minimize the statistical error of $P^{\mathrm{u}}(\xi)$. The global distribution is calculated by a weighted average of the distributions of the individual windows:

$$P^{\mathrm{u}}(\xi) = \sum_{i}^{\text{windows}} p_i(\xi) P_i^{\mathrm{u}}(\xi). \tag{14}$$

The weights p_i are chosen in order to minimize the statistical error of P^{u}:

$$\frac{\partial \sigma^2(P^{\mathrm{u}})}{\partial p_i} = 0 \tag{15}$$

under the condition $\sum p_i = 1$. This leads to[35,36]:

$$p_i = \frac{a_i}{\sum_j a_j}, a_i(\xi) = N_i \exp[-\beta\, \omega_i(\xi) + \beta F_i] \tag{16}$$

with N_i being the total number of steps sampled for window i. The F_i are calculated by Eq. (12):

$$\exp(-\beta F_i) = \int P^{\mathrm{u}}(\xi) \exp[-\beta w_i(\xi)]\, d\xi. \tag{17}$$

Because P^{u} enters Eq. (17) and F_i enters Eq. (14) via Eq. (16), these have to be iterated until convergence. For many bins, this convergence can be slow.

Umbrella Integration

An alternative to WHAM for combining the windows in umbrella sampling simulations with harmonic biases is umbrella integration.[37] The problem of calculating F_i is avoided by averaging the mean force rather than the distribution P. The unbiased mean force is independent of the F_i:

$$\frac{\partial A_i^{\mathrm{u}}}{\partial \xi} = -\frac{1}{\beta} \frac{\partial \ln P_i^{\mathrm{b}}(\xi)}{\partial \xi} - \frac{dw_i}{d\xi}. \tag{18}$$

The distribution P_i^{b} is expanded into a cumulant expansion, which is truncated after the second term (i.e., approximating P_i^{b} by a normal distribution). This is equivalent to truncating a power series of $A_i^{\mathrm{u}}(\xi)$ after the quadratic term. Because $A(\xi)$ can be assumed to be smooth and because each window is only supposed to cover a small part of ξ, truncating such a power expansion is well justified:

$$P_i^{\mathrm{b}}(\xi) = \frac{1}{\sigma_i^{\mathrm{b}}\sqrt{2\pi}} \exp\left[-\frac{1}{2}\left(\frac{\xi - \overline{\xi_i^{\mathrm{b}}}}{\sigma_i^{\mathrm{b}}}\right)^2\right]. \quad (19)$$

Thus, and with a bias in the form of Eq. (13), Eq. (18) now reads

$$\frac{\partial A_i^{\mathrm{u}}}{\partial \xi} = \frac{1}{\beta}\frac{\xi - \overline{\xi_i^{\mathrm{b}}}}{\left(\sigma_i^{\mathrm{b}}\right)^2} - K\left(\xi - \xi_i^{\mathrm{ref}}\right) \quad (20)$$

which only depends on the mean value $\overline{\xi_i^{\mathrm{b}}}$ and the variance $(\sigma_i^{\mathrm{b}})^2$ of ξ in each window. These two quantities can easily be sampled. For one window, before combining the different windows, its integration yields:

$$A_i^{\mathrm{u}}(\xi) = \frac{\left(\xi - \overline{\xi_i^{\mathrm{b}}}\right)^2}{2}\left(\frac{1}{\beta\left(\sigma_i^{\mathrm{b}}\right)^2} - K\right) + \left(\xi - \overline{\xi_i^{\mathrm{b}}}\right) K\left(\xi_i^{\mathrm{ref}} - \overline{\xi_i^{\mathrm{b}}}\right) + C_i. \quad (21)$$

$\overline{\xi_i^{\mathrm{b}}}$ shifts $A_i^{\mathrm{u}}(\xi)$ along the ξ axis and determines its slope, whereas $(\sigma_i^{\mathrm{b}})^2$ determines the curvature of A_i^{u}, and C_i is just the integration constant.

The curves of the mean forces of the different windows can directly be averaged to result in a global mean force:

$$\frac{\partial A}{\partial \xi} = \sum_i^{\text{windows}} p_i(\xi)\frac{\partial A_i^{\mathrm{u}}}{\partial \xi}. \quad (22)$$

This is conveniently done with (normalized) weights proportional to P_i^{b}:

$$p_i(\xi) = \frac{a_i}{\sum_j a_j}, \quad a_i(\xi) = N_i P_i^{\mathrm{b}}(\xi). \quad (23)$$

The resulting global mean force can be numerically integrated.

The difference between WHAM and umbrella integration is threefold: (1) The unbiased distributions of the images are averaged in WHAM, whereas the mean force is averaged in umbrella integration. (2) The biased distributions are approximated by normal distributions in umbrella integration, but not in WHAM. (3) The (non-normalized) weights for combining the windows are different: $a_i(\xi) = N_i \exp(-\beta w_i(\xi) + \beta F_i) = N_i P_i^{\mathrm{b}}/P_i^{\mathrm{u}}$ in WHAM and $a_i(\xi) = N_i P_i^{\mathrm{b}}$ in umbrella integration.

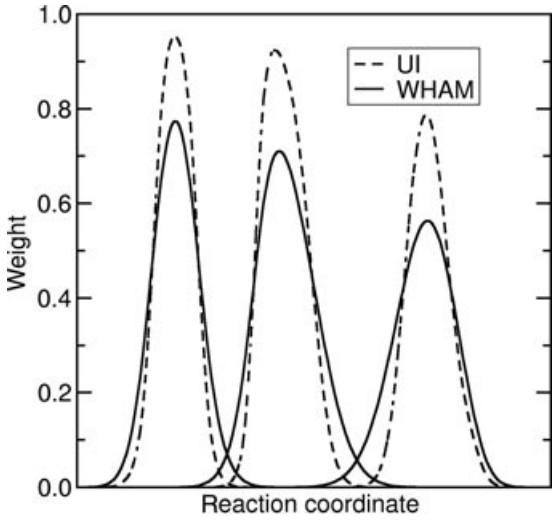

FIGURE 3 | Weights of weighted histogram analysis method (WHAM) and umbrella integration of three windows in a real simulation of the enzyme *para*-hydroxybenzoate hydroxylase (PHBH).[49] A maximum in the free energy is found between the second and third windows.

The first point is the main difference between the methods. The second difference can be changed in either of the methods. If umbrella integration is applied on the whole distribution, its noise level increases generally above the one obtained by WHAM. The additional differentiation adds to the noise. Also, its convergence properties with the bin width (number of bins) are lost. On the contrary, WHAM was meanwhile used with P_i^{b} approximated by normal distributions.[37,71] This leads to free-energy profiles as smooth as those obtained from umbrella integration.

The weights used by the different methods are somewhat difficult to transform between the methods because they weight different quantities. However, weights used in real simulations can be compared as depicted in Figure 3. In both cases, analytic quantities, not directly dependent on histograms, are used in a_i. Thus, the weights are smooth curves even if the distributions are noisy. It is clear from Figure 3 that the weights used in WHAM are broader than the ones used in umbrella integration. Using the weights of umbrella integration $a_i(\xi) = N_i P_i^{\mathrm{b}}$ in WHAM is possible, but it results in noisier curves because P_i^{b} is directly obtained from histograms in WHAM. It also leads to slightly deteriorated free-energy profiles as the windows effectively overlap less. Strong overlap

between the windows is more important in WHAM than in umbrella integration.

As a special case of umbrella integration, one can truncate the power series of $A(\xi)$ already after the linear term[19,37,72–75]:

$$\frac{\partial A_i^{\mathrm{u}}}{\partial \xi} = -K\left(\overline{\xi_i^{\mathrm{b}}} - \xi_i^{\mathrm{ref}}\right). \tag{24}$$

Comparison with Eq. (20) shows that this is accurate for $\xi = \overline{\xi_i^{\mathrm{b}}}$. However, it has also been used for $\xi = \xi_i^{\mathrm{ref}}$.

The expressions of umbrella integration allow for an estimate of the statistical error in ΔA from MD simulation data.[54] This, in turn, can be used to chose the parameters of the simulation, such as the strength of the bias K and the number of windows, in order to minimize the statistical error while keeping the requirement for CPU time at bay.

Umbrella integration can also be performed in multidimensional reaction coordinates.[76,77] However, the necessary integration step becomes more difficult (and prone to statistical error) in higher dimensions, whereas the alternative WHAM analysis can more straight forwardly be extended to more dimensions.

The main advantages of umbrella integration over WHAM are the independence of the number of grid points (bins) and the availability of an error estimate. The fact that only $\overline{\xi}$ and σ^2 enter the analysis of umbrella integration can be used to test the MD runs for equilibration[78] of these two quantities. This cannot directly be done for WHAM, where the whole distribution enters the analysis. However, in principle, one could test for equilibration of $\overline{\xi}$ and σ^2, and when these are equilibrated, assume that the whole distribution is equilibrated. Additionally, umbrella integration is noniterative, which speeds up the analysis. However, the CPU time required for the analysis is, in general, negligible as compared with the time needed to acquire the MD sampling data. The reduction of $A_i(\xi)$ to second order in ξ reduces noise significantly. For cases with very few windows, however, this can become a source of inaccuracies.

Estimation of the Sampling Error Bar

The error bar from finite sampling can be estimated using umbrella integration analysis.[54] This, in turn, allows to set up guidelines as to how the necessary simulation parameters should be set. The most important parameter is K, the strength of the bias. In general, K should be chosen as small as possible to allow for much overlap between the images. Let us introduce κ as the negative second derivative of the free energy with respect to ξ at the main barrier. Then, $K > \kappa$ is necessary to ensure a unimodular distribution in all images. This is necessary in umbrella integration because these distributions are approximated by normal distributions. In WHAM, sampling over the barrier is necessary, resulting in $K > \kappa - k_{\mathrm{B}}T$. Of course, κ is not known *a priori*, but sometimes it can be estimated.[54]

In general, it is preferable to sample many windows for shorter times than fewer windows for longer.[79] This leads to a smaller statistical error because of the better overlap between the windows and is better parallelizable.

CONCLUSION

The question whether umbrella sampling or one of its related methods discussed in *Accelerated Sampling Techniques* is to be used cannot be answered in general. It may depend on the particular system. Some authors have compared the applicability of some of these methods.[44,80–82] Although umbrella sampling might be preferred over thermodynamic integration because of errors in the integration[80] (which reduce with more windows), the additional free parameter K, which has to be chosen in umbrella sampling, was used as an argument against the latter.[82] Additionally, the availability of a correction of the metric tensor for the particular choice of the reaction coordinate might be an argument in favor of umbrella sampling, where such a correction is unnecessary.

Overall, umbrella sampling is meanwhile a mature and broadly accepted method for calculating free-energy differences.

ACKNOWLEDGMENTS

The author thanks the German Research Foundation (DFG) for financial support within the Cluster of Excellence in Simulation Technology (EXC 310/1) and grant SFB716/C.6, both at the University of Stuttgart.

REFERENCES

1. Arrhenius S. Über die Reaktionsgeschwindigkeit bei der Inversion von Rohrzucker durch Säuren. *Z Phys Chem (Leipzig)* 1889, 4:226–248.
2. Eyring H. The activated complex in chemical reactions. *J Chem Phys* 1935, 3:107–115.
3. Evans MG, Polanyi M. Some applications of the transition state method to the calculation of reaction velocities, especially in solution. *Trans Faraday Soc* 1935, 31:875–894.
4. Chandler D. Statistical mechanics of isomerization dynamics in liquids and the transition state approximation. *J Chem Phys* 1978, 68:2959–2970.
5. Kollman P. Free energy calculations: Applications to chemical and biochemical phenomena. *Chem Rev* 1993, 93:2395–2417.
6. Beveridge DL, DiCapua FM. Free energy via molecular simulation: Applications to chemical and biomolecular systems. *Annu Rev Biophys Biophys Chem* 1989, 18:431–492.
7. Christ CD, Mark AE, van Gunsteren WF. Basic ingredients of free energy calculations: A review. *J Comput Chem* 2010, 31:1569–1582.
8. Rosta E, Woodcock HL, Brooks BR, Hummer G. Artificial reaction coordinate "tunneling" in free-energy calculations: The catalytic reaction of RNase H. *J Comput Chem* 2009, 30:1634–1641.
9. Knight JL, Brooks III CL. λ-Dynamics free energy simulation methods. *J Comput Chem* 2009, 30:1692–1700.
10. Kong X, Brooks CL III. λ-Dynamics: A new approach to free energy calculations. *J Chem Phys* 1996, 105:2414–2423.
11. Liu Z, Berne BJ. Method for accelerating chain folding and mixing. *J Chem Phys* 1993, 99:6071–6077.
12. Tidor B. Simulated annealing on free energy surfaces by a combined molecular dynamics and Monte Carlo approach. *J Phys Chem* 1993, 97:1069–1073.
13. Laio A, Parrinello M. Escaping free-energy minima. *Proc Natl Acad Sci U S A* 2002, 99:12562–12566.
14. Torrie GM, Valleau JP. Monte Carlo free energy estimates using non-Boltzmann sampling: Application to the sub-critical Lennard-Jones fluid. *Chem Phys Lett* 1974, 28:578–581.
15. Torrie GM, Valleau JP. Nonphysical sampling distributions in Monte Carlo free-energy estimation: Umbrella sampling. *J Comput Phys* 1977, 23:187–199.
16. Born M. Volumen und Hydratationswärme der Ionen. *Z Phys* 1920, 1:45–48.
17. Kirkwood JG. Statistical mechanics of fluid mixtures. *J Chem Phys* 1935, 3:300–313.
18. Carter EA, Ciccotti G, Hynes JT, Kapral R. Constrained reaction coordinate dynamics for the simulation of rare events. *Chem Phys Lett* 1989, 156:472–477.
19. van Gunsteren WF. Methods for calculation of free energies and binding constants: successes and problems. In: van Gunsteren WF, Weiner PK, eds. *Computer Simulation of Biomolecular Systems*. Vol. 1 Leiden: ESCOM; 1989, 27.
20. Straatsma TP, McCammon JA. Multiconfiguration thermodynamic integration. *J Chem Phys* 1991, 95:1175–1188.
21. Sprik M, Ciccotti G. Free energy from constrained molecular dynamics. *J Chem Phys* 1998, 109:7737–7744.
22. Ciccotti G, Ferrario M. Blue moon approach to rare events. *Mol Sim* 2004, 30:787–793.
23. Ryckaert JP, Ciccotti G, Berendsen HJC. Numerical integration of the Cartesian equations of motion of a system with constraints: Molecular dynamics of n-alkanes. *J Comput Phys* 1977, 23:327–341.
24. Mülders T, Krüger P, Swegat W, Schlitter J. Free energy as the potential of mean constraint force. *J Chem Phys* 1996, 104:4869–4870.
25. Jain A. Compensating mass matrix potential for constrained molecular dynamics. *J Comput Phys* 1997, 136:289–297.
26. den Otter WK, Briels WJ. The calculation of free-energy differences by constrained molecular-dynamics simulations. *J Chem Phys* 1998, 109:4139–4146.
27. den Otter WK. Thermodynamic integration of the free energy along a reaction coordinate in cartesian coordinates. *J Chem Phys* 2000, 112:7283–7292.
28. Darve E, Pohorille A. Calculating free energies using average force. *J Chem Phys* 2001, 115:9169–9183.
29. Schlitter J, Klähn M. A new concise expression for the free energy of a reaction coordinate. *J Chem Phys* 2003, 118:2057–2060.
30. Schlitter J, Klähn M. The free energy of a reaction coordinate at multiple constraints: A concise formulation. *Mol Phys*, 2003, 101:3439–3443.
31. Hénin J, Chipot C. Overcoming free energy barriers using unconstrained molecular dynamics simulations. *J Chem Phys* 2004, 121:2904–2914.
32. Straatsma TP, Berendsen HJC, Postma JPM. Free energy of hydrophobic hydration: A molecular dynamics study of noble gases in water. *J Chem Phys* 1986, 85:6720–6727.
33. Beveridge DL, DiCapua FM. Free energy via molecular simulatin: a primer. In: van Gunsteren WF, Weiner PK, eds. *Computer Simulation of Biomolecular Systems*. Vol. 1. Leiden, The Netherlands: ESCOM; 1989, 1–26.
34. Hermans J. Simple analysis of noise and hysteresis in (slow-growth) free energy simulations. *J Phys Chem* 1991, 95:9029–9032.

35. Kumar S, Rosenberg JM, Bouzida D, Swendsen RH, Kollman PA. The weighted histogram analysis method for free-energy calculations on biomolecules. I. The method. *J Comput Chem* 1992, 13:1011–1021.
36. Souaille M, Roux B. Extension to the weighted histogram analysis method: Combining umbrella sampling with free energy calculations. *Comput Phys Commun*, 2001 135:40–57.
37. Kästner J, Thiel W. Bridging the gap between thermodynamic integration and umbrella sampling provides a novel analysis method: "Umbrella integration". *J Chem Phys* 2005, 123:144104(1–5).
38. Grubmüller H, Heymann B, Tavan P. Ligand binding and molecular mechanics calculation of the streptavidin-biotin rupture force. *Science* 1996, 271:997–999.
39. Izrailev S, Stepaniants S, Balsera M, Oono Y, Schulten K. Molecular dynamics study of unbinding of the avidin-biotin complex. *Biophys J* 1997, 72:1568–1581.
40. Evans E, Ritchie K. Dynamic strength of molecular adhesion bonds. *Biophys J* 1997, 72:1541–1555.
41. Balsera M, Stepaniants S, Izrailev S, Oono Y, Schulten K. Reconstructing potential energy functions from simulated force-induced unbinding processes. *Biophys J*, 1997, 73:1281–1287.
42. Jarzynski C. Nonequilibrium equality for free energy differences. *Phys Rev Lett* 1997, 78:2690–2693.
43. Hummer G. Fast-growth thermodynamic integration: Error and efficiency analysis. *J Chem Phys* 2001, 114:7330–7337.
44. Zuckerman DM, Woolf TB. Theory of a systematic computational error in free energy differences. *Phys Rev Lett* 2002, 89:180602–180606.
45. Bennett CH. Efficient estimation of free energy differences from Monte Carlo data. *J Comput Phys* 1976, 22:245–268.
46. Zwanzig RW. High-temperature equation of state by a perturbation method. I. Nonpolar gases. *J Chem Phys* 1954, 22:1420–1426.
47. Hu H, Yang W. Free energies of chemical reactions in solution and in enzymes with *ab initio* quantum mechanics/molecular mechanics methods. *Annu Rev Phys Chem* 2008, 59:573–601.
48. Zhang Y, Liu H, Yang W. Free energy calculation on enzyme reactions with an efficient iterative procedure to determine minimum energy paths on a combined *ab initio* QM/MM potential energy surface. *J Chem Phys* 2000, 112:3483–3493.
49. Kästner J, Senn HM, Thiel S, Otte N, Thiel W. QM/MM free-energy perturbation compared to thermodynamic integration and umbrella sampling: Application to an enzymatic reaction. *J Chem Theory Comput* 2006, 2:452–461.
50. Senn HM, Kästner J, Breidung J, Thiel W. Finite-temperature effects in enzymatic reactions—Insights from QM/MM free-energy simulations. *Can J Chem* 2009, 87:1322–1337.
51. McDonald IR, Singer K. Machine calculation of thermodynamic properties of a simple fluid at supercritical temperatures. *J Chem Phys* 1967, 47:4766–4772.
52. McDonald IR, Singer K. Examination of the adequacy of the 12–6 potential for liquid argon by means of Monte Carlo calculations. *J Chem Phys* 1969, 50:2308–2315.
53. Frenkel D, Smit B. *Understanding Molecular Simulation: From Algorithms to Applications*. 2nd ed. San Diego, CA: Academic Press; 2002.
54. Kästner J, Thiel W. Analysis of the statistical error in umbrella sampling simulations by umbrella integration. *J Chem Phys* 2006, 124:234106(1–7).
55. Grossfield A, Woolf TB. Interaction of tryptophan analogs with POPC lipid bilayers investigated by molecular dynamics calculations. *Langmuir* 2002, 18:198–210.
56. Mills M, Andricioaei I. An experimentally guided umbrella sampling protocol for biomolecules. *J Chem Phys* 2008, 129:114101(1–13).
57. Mezei M. Adaptive umbrella sampling: Self-consistent determination of the non-Boltzmann bias. *J Comput Phys* 1987, 68:237–248.
58. Hooft RWW, van Eijck BP, Kroon J. An adaptive umbrella sampling procedure in conformational analysis using molecular dynamics and its application to glycol. *J Chem Phys* 1992, 97:6690–6694.
59. Bartels C, Karplus M. Multidimensional adaptive umbrella sampling: Applications to main chain and side chain peptide conformations. *J Comput Chem* 1997, 18:1450–1462.
60. Bartels C, Karplus M. Probability distributions for complex systems: Adaptive umbrella sampling of the potential energy. *J Phys Chem B* 1998, 102:865–880.
61. Huber T, Torda AE, van Gunsteren WF. Local elevation: A method for improving the searching properties of molecular dynamics simulation. *J Comput Aided Mol Design* 1994, 8:695–708.
62. Hansen HS, Hünenberger PH. Using the local elevation method to construct optimized umbrella sampling potentials: Calculation of the relative free energies and interconversion barriers of glucopyranose ring conformers in water. *J Comput Chem* 2010, 31:1–23.
63. Hansen HS, Hünenberger PH. Ball-and-stick local elevation umbrella sampling: Molecular simulations involving enhanced sampling within conformational or alchemical subspaces of low internal dimensionalities, minimal irrelevant volumes, and problem-adapted geometries. *J Chem Theory Comput* 2010, 6:2622–2646.
64. Wu D. An efficient umbrella potential for the accurate calculation of free energies by molecular simulation. *J Chem Phys* 2010, 133:044115(1–9).

65. Sugita Y, Okamoto Y. Replica-exchange molecular dynamics method for protein folding. *Chem Phys Lett* 1999, 314:141–151.
66. Sugita Y, Kitao A, Okamoto Y. Multidimensional replica-exchange method for free-energy calculations. *J Chem Phys* 2000, 113:6042–6051.
67. Curuksu J, Zacharias M. Enhanced conformational sampling of nucleic acids by a new hamiltonian replica exchange molecular dynamics approach. *J Chem Phys* 2009, 130:104110(1–8).
68. Ferrenberg AM, Swendsen RH. New Monte Carlo technique for studying phase transitions. *Phys Rev Lett* 1988, 61:2635–2638.
69. Ferrenberg AM, Swendsen RH. Optimized Monte Carlo data analysis. *Phys Rev Lett* 1989, 63:1195–1198.
70. Roux B. The calculation of the potential of mean force using computer simulations. *Comput Phys Commun* 1995, 91:275–282.
71. Chakravorty DK, Kumarasiri M, Soudackov AV, Hammes-Schiffer S. Implementation of umbrella integration within the framework of the empirical valence bond approach. *J Chem Theory Comput* 2008, 4:1974–1980.
72. Van Eerden J, Briels WJ, Harkema S, Feil D. Potential of mean force by thermodynamic integration: Molecular-dynamics simulation of decomplexation. *Chem Phys Lett* 1989, 164:370–376.
73. Billeter SR, van Gunsteren WF. Computer simulation of proton transfers of small acids in water. *J Phys Chem A* 2000, 104:3276–3286.
74. Maragliano L, Fischer A, Vanden-Eijnden E, Ciccotti G. String method in collective variables: Minimum free energy paths and isocommittor surfaces. *J Chem Phys* 2006, 125:024106(1–15).
75. Maragliano L, Vanden-Eijnden E. Single-sweep methods for free energy calculations. *J Chem Phys* 2008, 128:184110(1–10).
76. Kästner J. Umbrella integration in two or more reaction coordinates. *J Chem Phys* 2009, 131:034109(1–8).
77. Kästner J, Sherwood P. The ribosome catalyses peptide bond formation by providing high ionic strength. *Mol Phys* 2010, 108:293–306.
78. Schiferl SK, Wallace DC. Statistical errors in molecular dynamics averages. *J Chem Phys* 1985, 83:5203–5209.
79. Beutler TC, van Gunsteren WF. The computation of a potential of mean force: Choice of the biasing potential in the umbrella sampling technique. *J Chem Phys* 1994, 100:1492–1497.
80. Czaplewski C, Rodziewicz-Motowidlo S, Liwo A, Ripoll DR, Wawak RJ, Scheraga HA. Molecular simulation study of cooperativity in hydrophobic association. *Protein Sci* 2000, 9:1235–1245.
81. Shirts MR, Pande VS. Comparison of efficiency and bias of free energies computed by exponential averaging, the Bennett acceptance ratio, and thermodynamic integration. *J Chem Phys* 2005, 122:144107(1–15).
82. Trzesniak D, Kunz APE, van Gunsteren WF. A comparison of methods to compute the potential of mean force. *Chem Phys Chem* 2007, 8:162–169.

